coatings

MDPI

Article

Prickly Pear Fruit Extract: Capping Agent for the Sol–Gel Synthesis of Discrete Titanium Dioxide Nanoparticles and Sensitizer for Dye-Sensitized Solar Cell

Radhika Rajendhiran [1,†], Raji Atchudan [2,†], Jayabal Palanisamy [1], Athinarayanan Balasankar [1], Tae Hwan Oh [2], Venugopal Deivasigamani [1,*] and Subramaniyan Ramasundaram [2,*]

[1] Department of Physics, Gobi Arts & Science College, Gobichettipalayam, Erode 638 543, Tamil Nadu, India
[2] School of Chemical Engineering, Yeungnam University, Gyeongsan 38541, Republic of Korea
* Correspondence: venugac.rdv@gmail.com (V.D.); ramasundaram79@hotmail.com (S.R.)
† These authors contributed equally to this work.

Abstract: Plant extracts have been utilized as an ecofriendly natural reducing agent for the synthesis of nanomaterials, including metal oxides. Prickly pear (opuntia) fruit extract (PPE) was used as a reducing agent for the sol–gel synthesis of titanium dioxide nanoparticles (TiO_2 NPs) and as a sensitizer for the TiO_2 NPs photoanode used in dye-sensitized solar cells (DSSCs). Ultraviolet-visible and infrared spectra, X-ray diffraction patterns, and scanning electron microscopic images were confirmed in the formation of semiconducting TiO_2 NPs with the predominate size of ~300 nm. The use of PPE rendered discrete TiO_2 NPs, whereas the typical synthesis without PPE resulted TiO_2 aggregates. TiO_2 NPs had a tetragonal crystalline structure, and their grain size was varied with respect to the concentration of PPE. The size of TiO_2 crystallites was found to be 20, 19, 15, and 10 nm when the volume percentage of PPE was 0.2, 0.4, 0.6, and 0.8%, respectively. TiO_2 NPs obtained using PPE were coated on indium-doped tin oxide substrates and sensitized with natural dye made up of PPE and synthetic dyes, namely rose Bengal (RB) and eosin yellow (EY). The photoanode fabricated with dye-sensitized TiO_2 NPs was subjected to current–voltage response studies. The maximum power-conversion efficiency, 1.4%, was recorded for photoanodes sensitized with PPE dye, which is considerably higher than that for RB (1.16%) or EY (0.8%). Overall, the above findings proved that PPE can be used as a potential reducing/capping agent and TiO_2 sensitizer for DSSC applications.

Keywords: prickly pear fruit; plant extract; titanium dioxide nanoparticles; sol–gel synthesis; dye-sensitized solar cell; photoanode

check for updates

Citation: Rajendhiran, R.; Atchudan, R.; Palanisamy, J.; Balasankar, A.; Oh, T.H.; Deivasigamani, V.; Ramasundaram, S. Prickly Pear Fruit Extract: Capping Agent for the Sol–Gel Synthesis of Discrete Titanium Dioxide Nanoparticles and Sensitizer for Dye-Sensitized Solar Cell. *Coatings* **2023**, *13*, 579. https://doi.org/10.3390/coatings13030579

Academic Editor: Keith J. Stine

Received: 15 February 2023
Revised: 3 March 2023
Accepted: 4 March 2023
Published: 7 March 2023

Copyright: © 2023 by the authors. Licensee MDPI, Basel, Switzerland. This article is an open access article distributed under the terms and conditions of the Creative Commons Attribution (CC BY) license (https://creativecommons.org/licenses/by/4.0/).

1. Introduction

A dye-sensitized solar cell (DSSC) is a vital power-generation device that has been considered as potential alternative to traditional silicon and thin film solar cell technologies. When compared with silicon and thin film solar cells, DSSC possesses advantages, such as lower manufacturing costs, fabrication under ambient conditions, better performance under diffused light conditions, and an ecofriendly nature [1,2]. Additionally, perovskite solar cells have shown promising results in recent years, but DSSCs have several advantages over them, including better stability, lower manufacturing costs, better performance under low light conditions, and a lower environmental impact in that they do not contain toxic lead–based materials that are commonly used in perovskite solar cells [3,4]. TiO_2 is the most common semiconductor being utilized in DSSC thanks to its nontoxic nature, availability at a low cost, and chemical stability. A thin film of TiO_2 nanoparticles (NPs) is used as an anode and immobilization site for dye molecules capable of harvesting visible light. TiO_2 transports the electrons generated upon light absorption by using a dye molecule. Though several methods are available, the sol–gel method has been considered as the ideal method for the synthesis of TiO_2 NPs. Sol–gel synthesis is simple, can be performed under

ambient conditions, and allows the tuning of the morphology via controlling the processing parameters. In the sol–gel synthesis, TiO_2 precursors, usually titanium(IV) isopropoxide, titanium(IV) butoxide, and titanium chloride, are subjected to acid hydrolysis. These titanium (Ti) precursors are sensitive to water and highly prone to undergoing hydrolysis. To control the rate of hydrolysis and the aggregation of TiO_2, acid catalysts, such as hydrochloric acid, nitric acid, and acetic acid, are used. These acid catalysts chelate with the Ti precursors and decrease the rate of hydrolysis [2,5–7]. In the nanomaterial synthesis, various plant extracts and microorganism are being used as either stabilizing/capping agents or reducing agents [8]. In some cases, together with acid catalysts, the natural extracts have been used as stabilizers, capping agents, or functional coatings [9].

In a green sol–gel synthesis, the acid catalysts have been completely replaced by plant part extracts. These green synthesis methods have emerged as versatile, ecofriendly, competent, and cost-effective for obtaining TiO_2 NPs. In typical green synthesis, first, an aqueous or ethanolic extract of plant parts is prepared, filtered, and added dropwise to the mixture of Ti precursor in water or ethanol. The TiO_2 NPs formed after stirring for a designated amount of time was separated, dried, and calcined [8]. Rajendhiran et al. synthesized homogenously distributed TiO_2 NPs (10–21 nm) by using 10 g/10 mL aqueous extract of the terminalia catappa (TC) and carissa carandas (CC) fruits. The constituents in the TC (gallic acid, brevifolin carboxylic acid, and ellagic acid) and CC (carissic acid, carisol, ascorbic acid, beta-sitosterol, ursolic acid, and lupeol) acted as capping agents [10]. An aqueous extract of the aloe vera plant (25 g/100 mL), containing minerals, vitamins, fatty acids, and amino acids, was also used for the sol–gel synthesis of TiO_2 NPs. Irregular TiO_2 NPs (60–80 nm) were obtained [11]. Fall et al. used an aqueous orange peel extract (25 g/400 mL) for TiO_2 synthesis; the addition of titanium (IV) bis (ammonium lactate) dihydroxide to the orange extract resulted in TiO_2 NPs with sizes in the 50–100 nm range [12]. Rodríguez-Jiménez et al. used leaf extracts for *Equisetum arvense*, *Syzygium aromaticum*, and *Camellia sinensis* for the sol–gel synthesis of TiO_2. The phenolic compounds in the plant extracts acted as surfactants and rendered discrete TiO_2 NPs (20–50 nm). These TiO_2 NPs were useful in biomedical, cosmetic, photocatalysis, and photovoltaic applications [13].

As far as the DSSC application is concerned, several plant extracts with natural dye characteristics coated the TiO_2 NPs, which were prepared by using a typical acid-catalyzed sol–gel synthesis. In most of the cases, the natural dye was first extracted from the plant; next, the extract was concentrated and coated on TiO_2 NPs [14,15]. Betanin-rich beetroot extract, brazilein pigment (containing a heartwood (*Caesalpinia sappan*) extract), anthocyanin-rich flower (hibiscus)/fruits (basella alba, scutia myrtina) extracts, carotene, anthocyanin (containing an extract of *Peltophorum pterocarpum*/*Acalypha amentacea* leaves), and turmeric were used for sensitizing TiO_2 NPs [16–21]. In multiple reports, prickly pear fruit (opuntia) extract (PPE), containing betacyanin and indicaxanthin, was used for sensitizing TiO_2 NPs. Because of the presence of carboxylic acid groups, these dyes can bind strongly on the surface of TiO_2 NPs. The natural dye from PPE (PP dye) was used to sensitize TiO_2 photoanodes, and this resulted in a 0.5%–1% power-conversion efficiency [21–26]. In addition to dye, PPE is also known to contain galacturonic acid [27]. Therefore, PPE extract is predicted as being capable of replacing acid catalysts in sol–gel synthesis and as being a natural dye for sensitizing the resultant TiO_2 NPs.

In the present investigation, first, an attempt is made to use PPE extract as an acid catalyst-free sol–gel synthesis of discrete TiO_2 NPs and as a natural dye sensitizer. The sol–gel synthesis of TiO_2 NPs was performed as a function of varying concentrations of aqueous PPE extract. Green synthesized TiO_2 NPs were heat treated, coated on the electrode, and sensitized with PP dye. TiO_2 NP samples were subjected to physicochemical characterization. DSSC was fabricated by using PP dye-sensitized TiO_2 NP photoanodes. For comparison, the synthetic dyes, rose Bengal (RB) and eosin yellow (EY), were also used for sensitizing green synthesized TiO_2 NPs. Thanks to following advantages, RB and EY were chosen for comparison over other commercially available dyes. RB and EY possess

high molar extinction coefficients and broad absorption spectra. They are thereby capable of absorbing large amounts of light compared with other dyes. These dyes are stable under ambient conditions, commercially available at lower costs, and nontoxic in nature [28,29].

2. Materials and Methods

2.1. Materials

Prickly pear fruits were collected from the surroundings of agricultural lands in Gobichettipalayam, Tami Nadu, India. Titanium tetra isopropoxide (TIP, Aldrich, St. Louis, MO, USA), ethanol (Merck, Rahway, NJ, USA) 99.9%, rose Bengal (RB, Alfa, Montgomery, AL, USA), eosin yellow (EY, Alfa), graphite plate (Alfa), chromic acid (H_2CrO_4), hydrochloric acid (HCl 98%, Merck), indium-doped tin oxide (ITO)-coated conductive glass substrate, glycerol (Sigma), sulfuric acid (H_2SO_4, Merck), potassium dichromate ($K_2Cr_2O_4$, Merck), acetone (C_3H_6O, Merck), ethylene glycol ($C_2H_6O_2$, Merck), potassium iodide (KI, Merck), and iodine (I, Merck) were used as purchased. Laboratory-created deionized water (DI water) was used for green synthesis and relevant analysis.

2.2. Preparation of Prickly Pear Fruit Extract (PPE)

Freshly harvested prickly pear fruits (30 g) were taken, thoroughly washed with DI water and cleaned by removing thorns and outer cover. The bright-red pulp was separated by removing the seeds and then was crushed into small pieces. The separated pulp (10 g) was mixed with 10 mL of DI water and allowed to remain at ambient temperature for 3 h. Next, the contents were heated to 60 °C and kept for 10 min. After heat treatment, the solid fruit pieces were removed by filtering through Whatman 41 filter paper. The resultant PPE (the filtrate) was used for synthesizing TiO_2 NPs.

2.3. Prickly Pear Dye Preparation

The freshly harvested prickly pear fruits (30 g) were cleaned with DI water as mentioned above and cut into small pieces. The pieces were subjected to manual crushing and squeezing, using mortar and pestle. The solid fragments were then removed by filtration and centrifugation (100 rpm, 15 min, twice). Afterward, 10 mL of extract (the supernatant) was taken and dissolved in 30 mL of 2:1 volume/volume mixture of ethanol and water. The pH value of the prepared PPE dye was found to be around 6.5–7. In order to use the pear for the further sensitization of TiO_2 NPs, the resultant PPE dye was stored in the dark.

2.4. Green Sol–Gel Synthesis of TiO_2 NPs

First, 100 mL of ethanol was added dropwise into 6 mL of TIP, and the mixture was continuously stirred for 2 h. Next, PPE was gradually added to this mixture while continuously stirring. The volume percentage of PPE varied between 0.2 and 0.8 with respect to the volume of TIP. After PPE addition, the contents were further stirred for 80 min and kept aside for 24 h. Afterward, the contents were filtered out, dried at 60 °C for 10 min, and heat treated using a muffle furnace set at 450 °C for 2 h. The resultant TiO_2 NPs was collected and stored in a glass container. A set of TiO_2 NP samples was prepared by adding 0.2%, 0.4%, 0.6%, and 0.8% of PPE; these sample were coded as PP2, PP4, PP6, and PP8, respectively.

2.5. Fabrication of DSSC Using Green Synthesized TiO_2 NPs

Figure 1 shows the steps involved in the fabrication of DSSC. To the green synthesized TiO_2 NPs powder (0.5 g), 0.2 mL of glycerol was added, and after, it was well ground into paste. This paste was coated on the ITO substrate (1 cm^2), cleaned by sonicating it with DI water and ethanol. The doctor blade coating method was followed. To control the thickness, 0.5 mm thick Scotch tape was fixed on the ITO substrate. To evaporate out the solvents, the TiO_2 NPs coated with ITO substrate were kept in the muffle furnace at 200 °C for 2 h. After drying, the TiO_2 NPs coated with ITO substrates were sensitized by separately soaking them in the dye solutions (0.5 mM RB dye, 0.5 mM EY, and PP

dye) for 12 h. The counter electrode construction contains a small volume of graphite plate that has been gradually scrubbed on the top of the ITO plate till the layer is uniform throughout the selected area. The dye-coated TiO_2 NP photoanode and the graphite-coated ITO cathode were kept opposite and bounded using binder clips. Electrolyte solution was prepared using a mixture of $C_2H_6O_2$ (10.5 mL), I (0.128 g), and KI (0.82 g), which was allowed to diffuse in between the anode and the cathode, prior to taking the current–voltage (I–V) measurement.

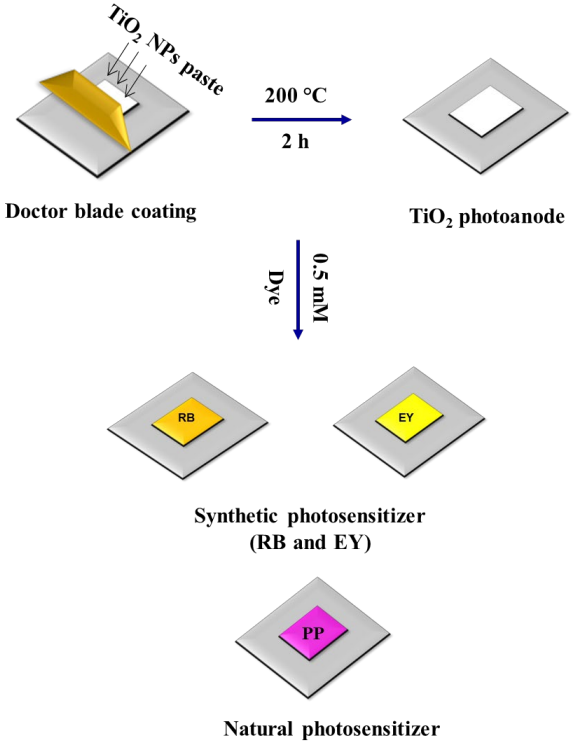


Figure 1. Steps involved in the fabrication of DSSC using green synthesized TiO_2 NPs.

2.6. Characterization

The crystalline structure of the TiO_2 NPs was studied using X-ray diffraction (XRD) patterns obtained with Rigaku XRD 600 X-ray diffractometer. The radiation source was Cu-Kα (λ = 1.54 Å). The surface morphology and surface elemental composition of the TiO_2 NP coating was assessed by using a scanning electron microscope (SEM, JEOL JSM6390) equipped with the energy dispersive X-ray spectrometer (EDXS). Fourier-transform infrared (FT−IR) spectra (400–4000 nm) were recorded with a Shimadzu (IR prestige21) FT−IR spectrophotometer. Ultraviolet-visible (UV-Vis) spectra were recorded using Shimadzu 1800 UV-Vis spectrophotometer. The current–voltage (I–V) studies for the DSSC were performed with a Keithley 2401 source meter under stimulated solar irradiation (Xenon arc lamp, 100 mW/cm^2).

3. Results and Discussion

XRD patterns of green synthesized TiO_2 NP samples (PP2, PP4, PP6, and PP8) are shown in Figure 2. The XRD patterns exhibited the characteristics diffraction peaks of TiO_2 at 25.25°, 37.88°, 47.86°, 54.78°, 62.92°, 70.25°, and 74.94°, corresponding to (101), (004), (200), (211), (204), (116), and (215) planes, respectively. These peaks were attributed to the tetragonal crystalline structure with lattice constants where a = 0.3784 and c = 0.9514; they were in close agreement with the anatase crystalline phase of TiO_2 [28–31]. The average size of the crystalline grains calculated using the Debye–Scherrer formula, on the basis of the most intense diffraction peak (101) [32], was 20, 19, 15, and 10 nm for PP2, PP4, PP6, and PP8, respectively. An increase in the volume of PPE during synthesis decreased the

average size of the crystalline grains from 20 to 10 nm. The reduction in the crystalline size was attributed to the increase in the nucleation density of the TiO_2 domains in response to the increase in the volume of PPE.

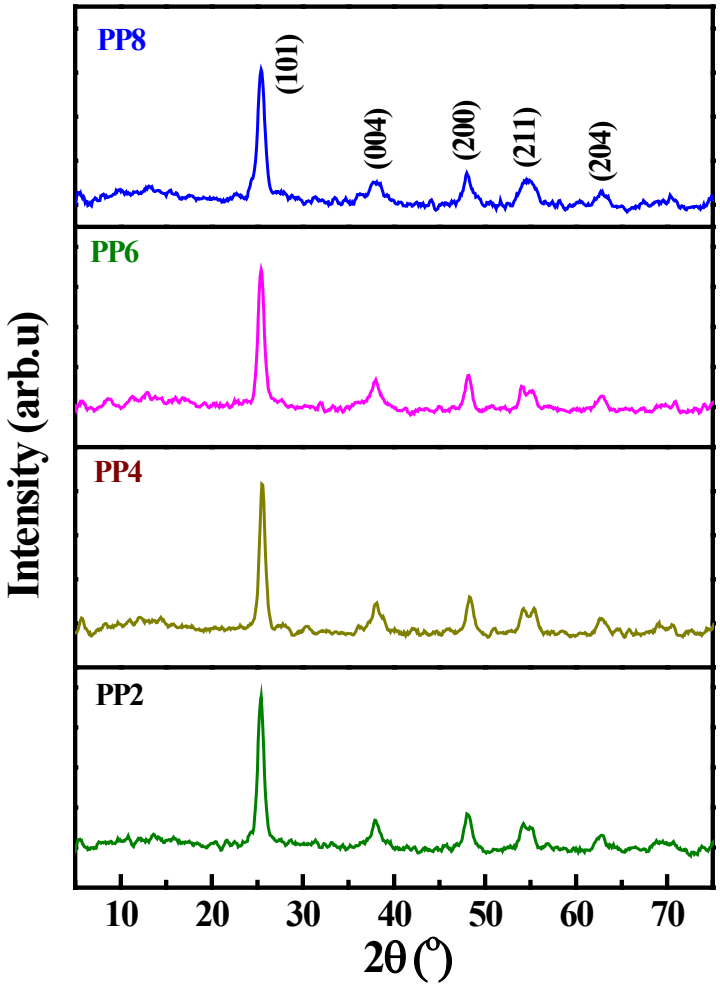


Figure 2. XRD pattern of green synthesized TiO_2 NP samples obtained as a function of varying volumes of PPE.

A similar trend was noticed in the earlier reports that dealt with the natural extract-assisted synthesis of TiO_2 NPs. In brief, the average size of the chemically synthesized TiO_2 crystallites was in the range of 20–22 nm, while the plant-extract-assisted synthesis caused a decrease in the average size of the TiO_2 crystallites to 9–15 nm. An increase in the number of capping molecules, the PPE, led to the effective stabilization of tiny nucleated TiO_2 domains, restricted coalescence, and prevented their growth [9,10]. Thus, the size of the crystallites declined in response to the increase in the volume of PPE.

Figure 3a–d shows the SEM image of green synthesized TiO_2 NP samples prepared as a function of varying volumes of PPE. All the green synthesized TiO_2 NP samples appeared to be spherical in shape. The size of particles remarkably decreased with an increase in the volume of PPE. In PP2, TiO_2 NPs were coalesced and had grown large in size. Though aggregates were found, the overall sizes of the TiO_2 NPs decreased when the volume of PPE increased. In particular, discrete particles were found in PP8. The overall sizes of the particles observed in these samples were 330 nm–1.66 µm in PP2, 306 nm–1.66 µm in PP4, 322 nm–1.35 µm in PP4, and 270 nm–1.35 µm in PP8. The populations of NPs increased with an increase in the volume of PPE used. Among all, a higher number of NPs was found in PP8. In XRD (Figure 2), where the size of the crystallizes decreased with an increase in the volume of PPE, similar sizes of TiO_2 particles decreased and became

discrete. The changes in particle size as a function of PPE concentration (sample code) was depicted in Figure 3e. The average particle size decreased from 841 to 675 nm when the concentration of PPE (%) to TiO_2 precursor (TIP) volume increased from 0.2% (PP2) to 0.8% (PP8), respectively. This observation confirmed the role of PPE extract as a stabilizer that largely prevented the agglomeration of TiO_2 NPs.

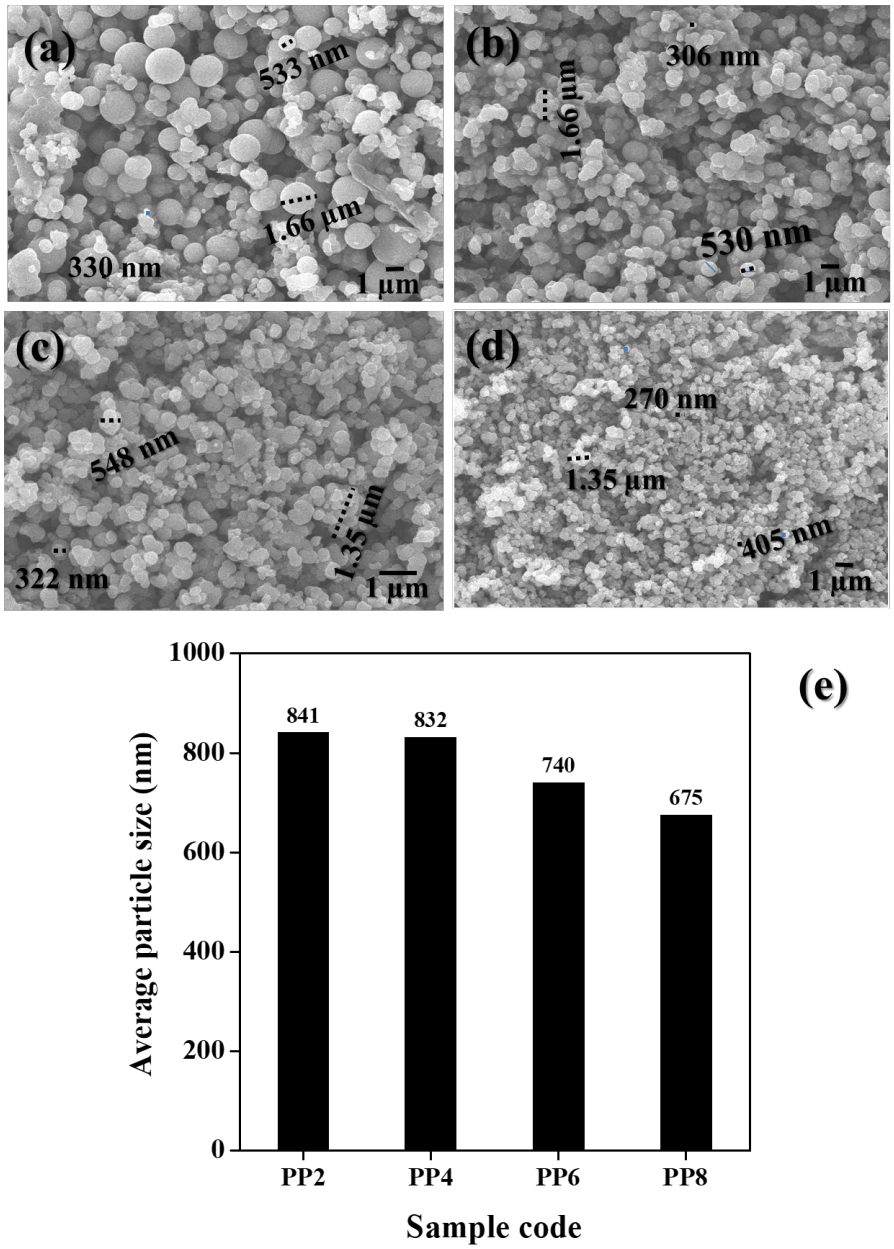


Figure 3. SEM images of green synthesized TiO_2 NPs: (**a**) PP2, (**b**) PP4, (**c**) PP6, and (**d**) PP8. (**e**) Bar chart indicating the average size of TiO_2 NPs.

The EDX spectra of describing the surface chemical composition of TiO_2 NPs are shown in Figure 4. The composition of the weight percentage (wt%) of Ti was in a range from 41.62% to 51.40%, and oxygen (O) was 48.60% to 52.14%. In all the samples, the relative composition of O was higher than the actual composition of O (equal to 66.85% of Ti content) in TiO_2. The excessive O content was associated with the concomitant oxygen species. Thus, the findings of EDX spectra also confirmed that PPE was useful for the green synthesis of TiO_2 NPs.

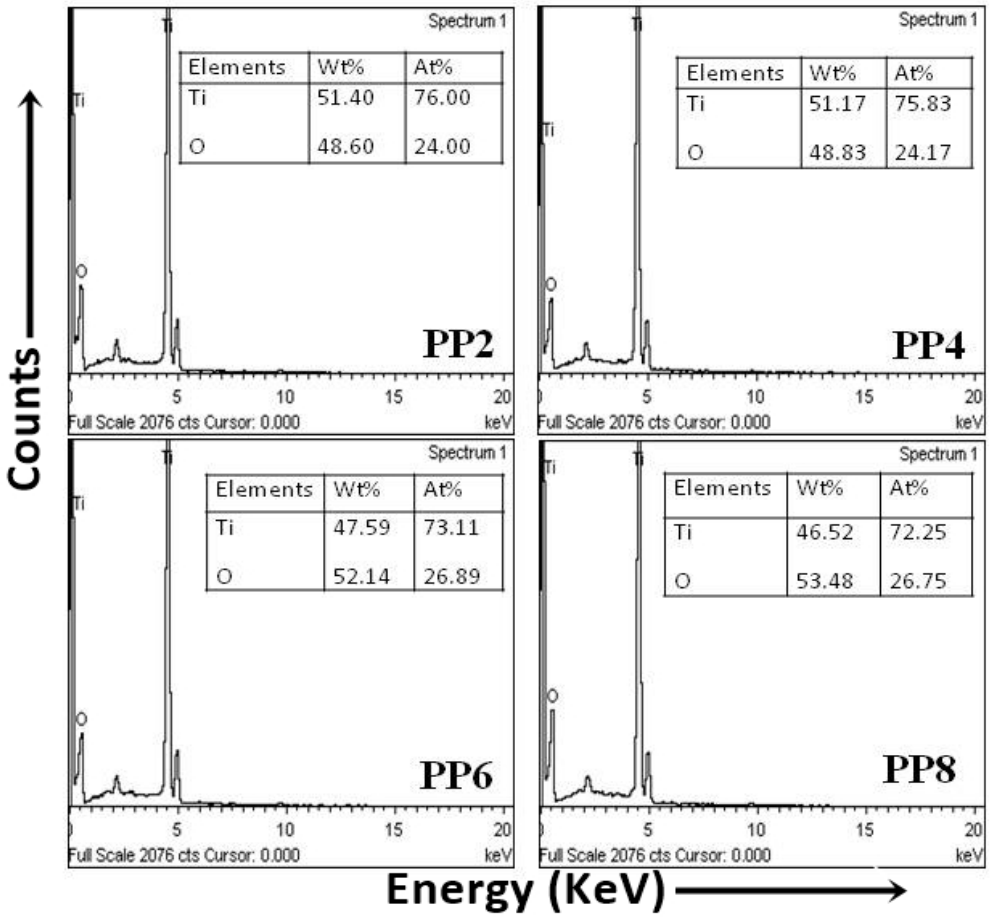


Figure 4. EDX spectra of green synthesized TiO_2 NPs.

Figure 5 shows the FT−IR spectra of the TiO_2 NP samples. Invariably, all exhibited IR peaks corresponding to the Ti–O stretching and O–Ti–O bridge stretching of TiO_2 between 1000–500 cm^{-1}. The peak in this region was Ti–O–Ti. The OH peaks associated with TiO_2 emerged at around 3400 cm^{-1}. The IR transmittance peaks found at 2900 (–CH_2 stretching), 1550 (C=C stretching), and 1400 cm^{-1} (–CH_3 bending) were attributed to the organic capping molecules present in PPE [9]. The peaks corresponding to the organic molecules were less pronounced in that the large portion of the plant-derived organic capping agents were highly prone to removal during the calcination process [13].

Figure 6a shows the UV-Vis spectra of the representative TiO_2 NPs: PP2 and PP8. These samples exhibited typical major electronic absorption of TiO_2 below 350 nm. There was weak absorption in the visible region between 350 and 600 nm, attributed to the remanence of the organic capping molecules in PPE after calcination. This observation was consistent with the UV-Vis spectrum of PPE reported in the literature. Figure 6b shows the absorption spectra of neat EY, RB, and PPE dyes. The dye exhibited absorption maxima at 537, 558, and 515 nm for EY, RB, and PPE dyes respectively. The absorption maxima observed for PPE dye was attributed to the beta cyan present in the extract. Additionally, it is seen that the PPE dye has broad absorption, compared with EY and RB indicates the conversion of more photons into current as it covers most of the visible spectrum leading to higher efficiency during the device formation [23].

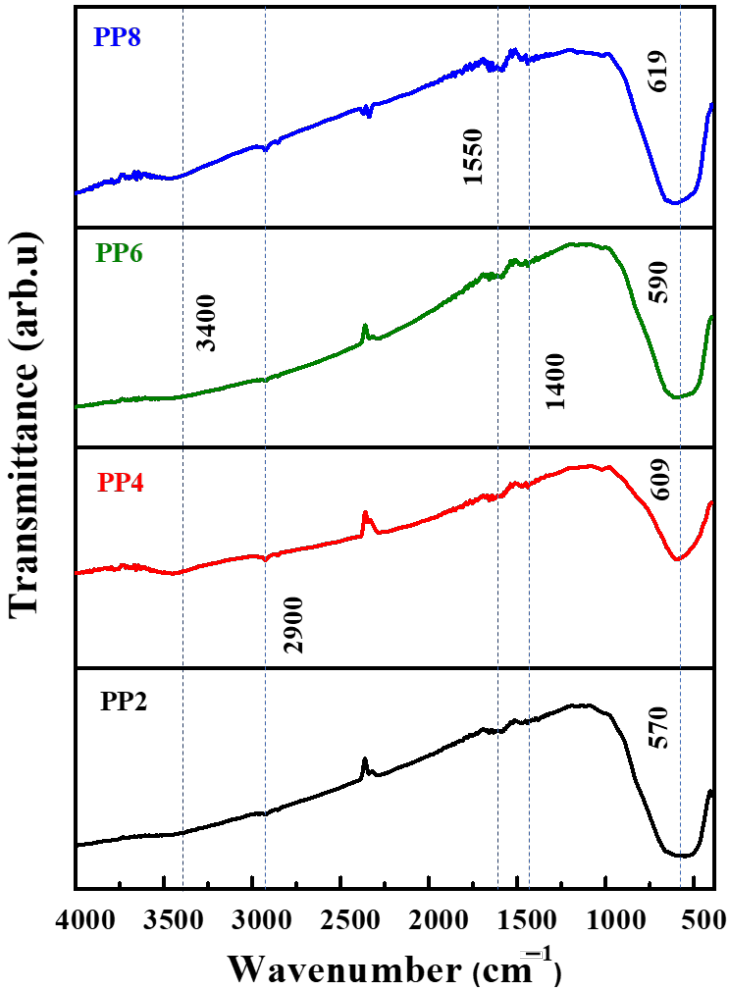


Figure 5. FT−IR spectra of green synthesized TiO_2 NP samples.

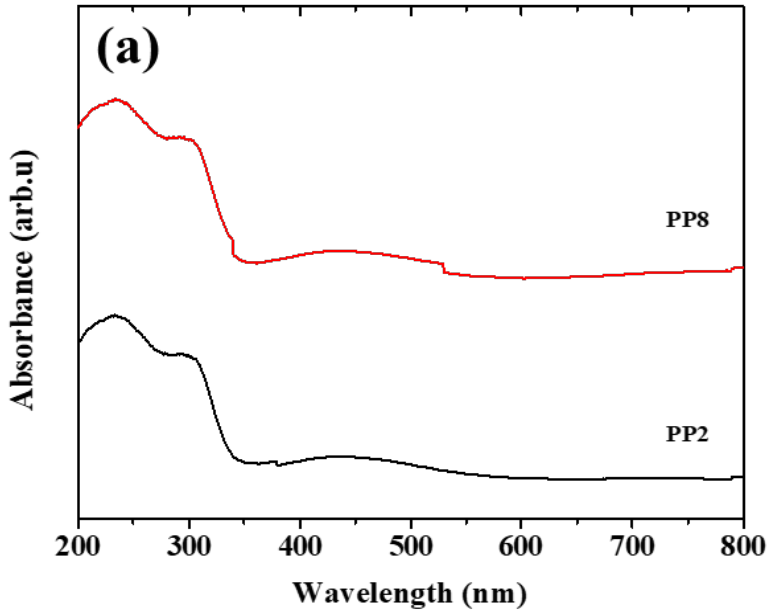


Figure 6. *Cont.*

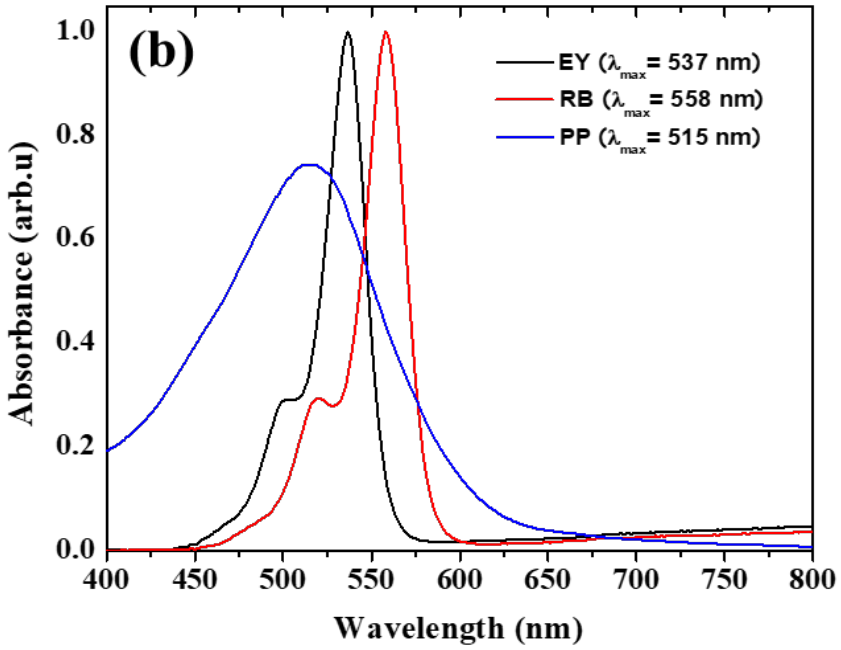


Figure 6. (**a**). UV-Vis spectra of representative green synthesized TiO_2 NPs samples, PP2, and PP8, (**b**) UV-Vis spectra of EY, RB and PP dyes.

Figure 7 shows the Tauc plot meant for drawing optical band-gap energy (E_g) from UV-Vis spectra. The following Tauc's equation was used for evaluating E_g:

$$(\alpha h\upsilon) = A(h\upsilon - E_g)\, n \quad (1)$$

where A is a photonic energy independent constant; h is the Planck constant; υ is the frequency of the photon; α is the absorption coefficient; and n depends on the type of transition (n = 1/2 for indirect transition and n = 2 for direct transition) [33–35]. According to this, the E_g values of PP2 and PP8 were 3.02 and 2.91 eV, respectively, slightly lower than the actual E_g of typical TiO_2 NPs, 3.14–3.24 eV [36,37].

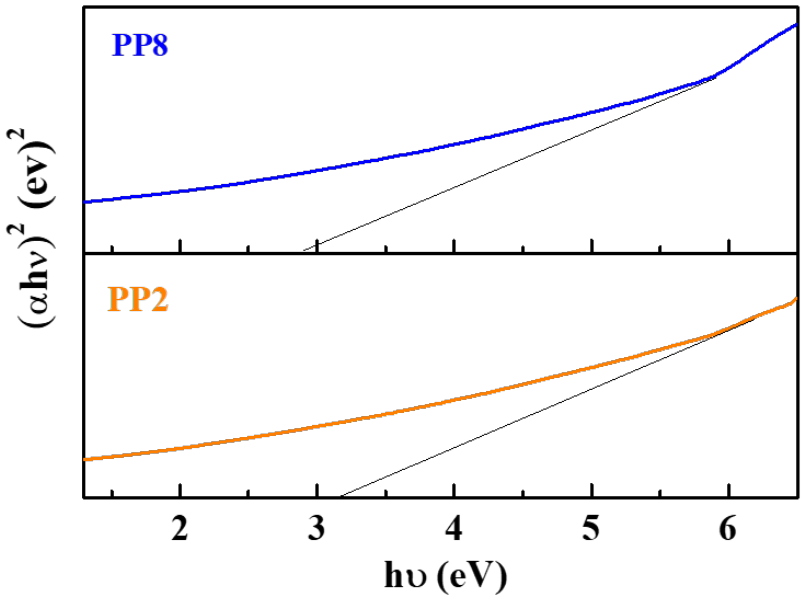


Figure 7. Band gap of representative green synthesized TiO_2 NPs samples (PP2 and PP8).

Figure 8 shows the J-V characteristics of DSSC sensitized with RB dye. The photovoltaic performances of DSSCs were calculated according to the fill factor (FF) and power-conversion efficiency (η), by using the following equations:

$$FF = V_m \times J_m / V_{oc} \times J_{sc} \quad (2)$$

$$\eta = V_{oc} \times J_{sc} \times FF / P_{in} \quad (3)$$

where V_m is the voltage at the maximum power point in volts, J_m is the maximum current density at maximum power point (mA cm^{-2}), V_{oc} is the open-circuit voltage in volts, J_{sc} is the short-circuited current density (mA cm^{-2}), and P_{in} is the incident light power radiation. It can be noted that the efficiency and the fill factor for the RB-sensitized samples increase with an increase in the concentration of PPE during synthesis. The obtained J-V parameters for the fabricated DSSCs are shown in Table 1.

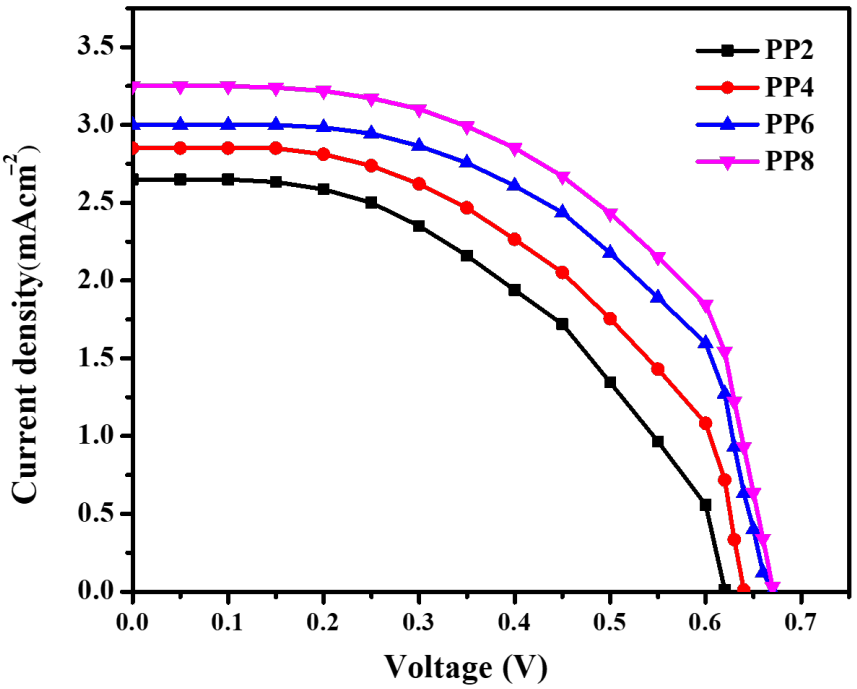


Figure 8. J−V characteristics of DSSC fabricated using TiO_2 NPs sensitized with RB.

Table 1. J−V characteristics of DSSC fabricated using the RB, EY, and PPE dyes.

Sample Codes	Dye	V_{oc} (V)	J_{sc} (mA cm^{-2})	FF%	η %
PP2	RB	0.61	2.64	0.47	0.75
PP4	RB	0.63	2.85	0.49	0.87
PP6	RB	0.66	2.99	0.53	1.04
PP8	RB	0.66	3.22	0.55	1.16
PP8	EY	0.64	2.85	0.48	0.80
PP8	*PP*	0.66	3.49	0.61	1.40

The maximum efficiency for the PP8 sample was observed thanks to sensitization of discrete TiO_2 NPs. The presence of discrete TiO_2 NPs favored an increase in the effective surface area and exerted a direct influence on the dye loading as well as on the efficiency of DSSCs. The efficiency of DSSC made by sensitizing the PP8 sample with EY, RB, and PPE dyes is shown in Table 1 and Figure 9.

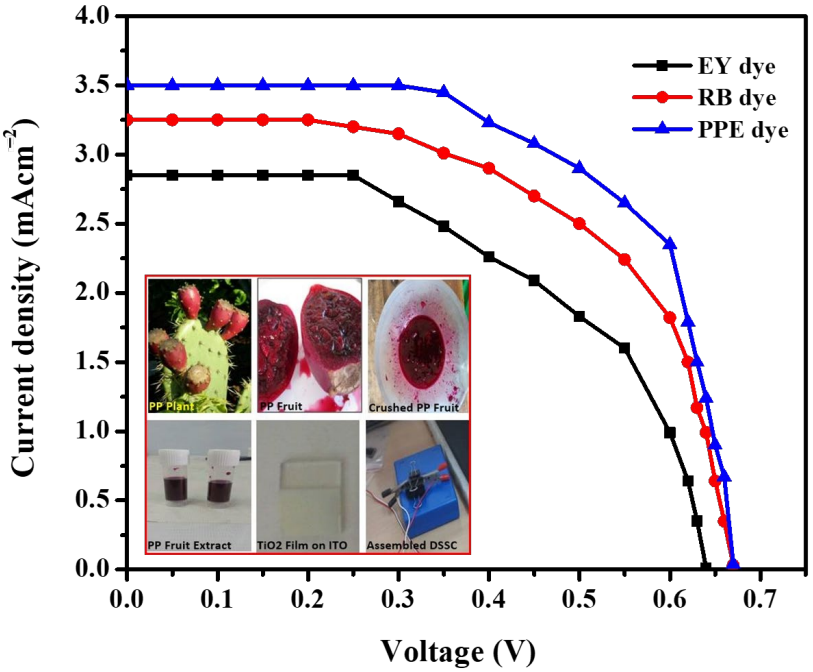


Figure 9. J−V characteristics of DSSC fabricated using TiO_2 NPs sensitized with RB, EY (synthetic dyes), and PP (natural dye). (Inset: photograph of PPE, PPE dye, and assembled device).

The reported power-conversion efficiencies of DSSC, where synthetic dyes RB, EY, and bromophenol blue sensitized the TiO_2 NP photoanodes used, are provided in Table 2. These values were considerably lower than the power-conversion efficiency value observed for DSSC fabricated with photoanodes made up of natural PP-dye-sensitized TiO_2 NPs that were obtained by using a PPE-assisted green sol–gel synthesis. The low efficiency obtained for the EY- and RB-dye-sensitized DSSCs compared to PP dye due to the low current density.

Moreover, the PP dye found to have the greatest ability to inject high electrons thereby increased the maximum current density. The J_{sc} is directly proportional to the number of dye molecules adsorbed into the working electrode because they produce electrons by absorbing light radiation or photoinduced electrons. The maximum dye loading and conversion efficiency exhibited by a PP-dye-sensitized DSSC was due to the firm anchoring of the PP dye on the TiO_2 NPs [37–40]. The presence of functional groups, such as hydroxyl and carbonyl groups in PP dye, favored the firm anchoring of the PP dye on TiO_2 NPs. The robust anchoring of dye molecules on TiO_2 NPs also minimized the charge carrier recombination and rendered the maximum efficiency. However, the observed efficiency was low compared to the N719 dye, owing to the minimum absorbance of sunlight [41–43].

Table 2. Comparison of efficiency of DSSC fabricated using PPE dye with the relevant literature.

Photo Anode	Dye	Efficiency (η%)	Reference
TiO_2	RB	0.89	[44]
TiO_2	RB	0.14	[45]
TiO_2 + ZnO	EY	0.39	[46]
TiO_2	EY	0.9	[29]
TiO_2	EY	1.07	[47]
TiO_2	EY	0.89	[48]
TiO_2	Bromophenol blue	0.33	[48]
PP8	RB	1.16	This work
PP8	EY	0.80	This work
PP8	PPE	1.40	This work

4. Conclusions

TiO_2 NPs were obtained by PPE-mediated green sol–gel synthesis. XRD patterns confirmed the green synthesis of TiO_2 NPs in the anatase crystalline phase, and the average crystallite size was in the range 20–10 nm. TiO_2 NPs were spherical in shape, and the major surface elemental constituents were Ti and O. The TiO_2 NPs synthesized using 8 mL of custom-made PPE rendered discrete TiO_2 NPs thanks to the stabilizing/capping effect of the organic molecules present in PPE. According to the UV-Vis spectra, the direct band gap (E_g) of TiO_2 NPs synthesized using 8 mL of PPE decreased from 3.2 to 2.91 eV. The PP dye extracted from prickle pear fruit was used as a natural dye photosensitizer. The DSSC fabricated by using PP-dye-sensitized TiO_2 NP photoanodes exhibited the maximum power-conversion efficiency (1.4%), higher than the DSSC fabricated by using TiO_2 NPs sensitized with synthetic dyes, specifically RB (1.16%) and EY (0.8%). Overall, PPE was found to be advantageous because PPE proved to be a good replacement for an acid catalyst as well as a synthetic capping agent used in the sol–gel synthesis of TiO_2 NPs. Additionally, when used as a sensitizer for TiO_2 NP photoanodes in DSSC, the PPE dye exhibited higher power-conversion efficiency compared with the low-cost synthetic dyes (RB and EY). These findings suggest that PPE could be used as an environmentally benign and low-cost functional resource for the sol–gel synthesis of metal oxide nanomaterials and sensitization meant for imparting visible light absorption.

Author Contributions: Conceptualization, data curation, formal analysis, and writing—original draft, R.R.; formal analysis and visualization, R.A.; investigation and visualization, J.P.; writing—review and editing, A.B. and T.H.O.; supervision, V.D.; conceptualization, writing—review and editing, S.R. All authors have read and agreed to the published version of the manuscript.

Funding: The authors R.R., J.P., A.B. and V.D. acknowledge the DST Gov. of India for the Common Instrumentation facility under the FIST grant (SRF/FST/College-2018-302 (C)). T.H.O. and S.R. acknowledge support by the National Research Foundation of Korea (NRF) grant funded by the Korea government (MSIT) (No. 2022R1A2C1004283) and by the Korea Basic Science Institute (National research Facilities and Equipment Center) grant funded by the Ministry of Education (2019R1A6C1010046).

Institutional Review Board Statement: Not applicable.

Informed Consent Statement: Not applicable.

Data Availability Statement: Upon reasonable request, the data supporting this investigation are available from the corresponding authors.

Acknowledgments: All authors acknowledge the support of Common Instrumentation facility at Gobi Arts & Science College, Gobichettipalayam, Erode, Tamilnadu, India—638 543.

Conflicts of Interest: The authors declare no conflict of interest.

References

1. Akila, Y.; Muthukumarasamy, N.; Velauthapillai, D. Chapter 5-TiO_2-based dye-sensitized solar cells. In *Nanomaterials for Solar Cell Applications*; Thomas, S., Kalarikkal, N., Wu, J., Sakho, E.H.M., Oluwafemi, S.O., Eds.; Elsevier: Amsterdam, The Netherlands, 2019; pp. 127–144. [CrossRef]
2. Jiawei, G.; Sumathy, K.; Qiquan, Q.; Zhengping, Z. Reiew on dye–sensitized solar cells (DSSC): Advanced techniques and research trends. *Renew. Sustain. Energy Rev.* **2017**, *68*, 234–246. [CrossRef]
3. Li, R.; Li, C.; Liu, M.; Vivo, P.; Zheng, M.; Dai, Z.; Zhan, J.; He, B.; Li, H.; Yang, W.; et al. Hydrogen-bonded dopant-free hole transport material enables efficient and stable inverted perovskite solar cells. *CCS Chem.* **2022**, *4*, 3084–3094. [CrossRef]
4. Wang, C.; Liu, M.; Rahman, S.; Pekka Pasanen, H.P.; Tian, J.; Li, J.; Deng, Z.; Zhang, H.; Vivo, P. Hydrogen bonding drives the self-assembling of carbazole-based hole-transport material for enhanced efficiency and stability of perovskite solar cells. *Nano Energy* **2022**, *101*, 107604. [CrossRef]
5. Macwan, D.P.; Dave, P.N.; Chaturvedi, S. A review on nano-TiO_2 Sol-gel type syntheses and its applications. *J. Mater. Sci.* **2011**, *46*, 3669–3686. [CrossRef]
6. Akpan, U.G.; Hameed, B.H. The advancements in sol-gel method of doped–TiO_2 photocatalysts. *Appl. Catal. A Gen.* **2010**, *375*, 1–11. [CrossRef]
7. Galkina, O.L.; Vinogradov, V.V.; Agafonov, A.V.; Vinogradov, A.V. Surfactant-Assisted Sol-Gel Synthesis of TiO_2 with Uniform Particle Size Distribution. *J. Inorg. Chem.* **2011**, *8*, 108087. [CrossRef]

8. Babu, N.; Pathak, V.M.; Singh, A.; Navneet, A. *Sonchus asper* leaves aqueous extract mediated synthesis of Titanium dioxide nanoparticles. *Pharma Innov. J.* **2019**, *8*, 817–822.
9. Nabi, G.; Khalid, N.R.; Tahir, M.B.; Rafique, M.; Rizwan, M.; Hussain, S.; Iqbal, T.; Majid, A. A Review on Novel Eco-Friendly Green Approach to Synthesis TiO_2 Nanoparticles Using Different Extracts. *J. Inorg. Organomet. Polym. Mater.* **2018**, *28*, 1552–1564. [CrossRef]
10. Radhika, R.; Venugopal, D.; Jayabal, P.; Saravanakumar, M.; Selvakumar, P. Terminali acatappa and carissacarandas assisted synthesis of TiO_2 nanoparticles—A green synthesis approach. *Mater. Today Proc.* **2021**, *45*, 2232–2238. [CrossRef]
11. Ganapathi Rao, K.; Ashok, C.H.; Venkateswara Rao, K.; Shilpa Chakra, C.H.; Tambur, P. Green Synthesis of TiO_2 Nanoparticles Using Aloe Vera Extract. *Int. J. Adv. Res. Phys. Sci.* **2015**, *2*, 28–34.
12. Fall, A.; Ngom, I.; Bakayoko, M.; Sylla, N.F.; Mohamed, H.E.; Jadvi, K.; Kaviyarasu, K.; Ngom, B.D. Biosynthesis of TiO_2 nanoparticles by using natural extract of Citrus sinensis. *Mater. Today Proc.* **2021**, *36*, 349–356. [CrossRef]
13. Rodríguez-Jiménez, R.A.; Panecatl-Bernal, Y.; Carrillo-López, J.; Méndez-Rojas, M.Á.; Romero-López, A.; Pacio-Castillo, M.; Vivaldo, I.; Morales-Sánchez, A.; Arce, R.D.; Caram, J.; et al. Influence of ethanolic plant extraction morphology and size distribution of sol-gel prepared TiO_2 nanoparticles. *Chem. Sel.* **2021**, *6*, 3958–3968. [CrossRef]
14. Richhariya, G.; Kumar, A.; Tekasakul, P. Natural dyes for dye sensitized solar cell: A review. *Renew. Sustain. Energy Rev.* **2017**, *69*, 705–718. [CrossRef]
15. Jamalullail, N.; Mohamad, I.S.; Norizan, M.N.; Baharum, N.A. Short review: Natural pigments photo sensitizer for dye-sensitized solar cell (DSSC). In Proceedings of the 2017 IEEE 15th Student Conference on Research and Development (SCOReD), Wilayah Persekutuan Putrajaya, Malaysia, 13–14 December 2017; pp. 344–349. [CrossRef]
16. Ananth, S.; Arumanayagam, T.; Vivek, P.; Murugakoothan, P. Direct synthesis of natural dye mixed titanium dioxide nanoparticles sol-gel method for dye sensitized solar cell applications. *Optik* **2014**, *125*, 495–498. [CrossRef]
17. Ananth, S.; Vivek, P.; Arumanayagam, T.; Murugakoothan, P. Pre dye treated titanium dioxide nanoparticles synthesized by modified sol-gel method for efficient dye-sensitized solar cells. *Appl. Phys. A* **2015**, *119*, 989–995. [CrossRef]
18. Swathi, S.; Kulkarani, S.; Hussaini, S.; Gajanan Bodkhe, A. Natural hibiscus dye and synthetic organic eosin dye sensitized solar cell using titanium dioxide nanoparticles photo anode: Comparative study. *Surf. Rev. Lett.* **2019**, *26*, 1850164. [CrossRef]
19. Sanjay, P.; Deep, K.; Mdhavan, J.; Senthil, S. Performance of TiO_2 based sensitized solar cells fabricated with dye extracted from leaves of peltophorum pterocarpum and acalypha amentacea as sensitizer. *Mater. Lett.* **2018**, *219*, 158–162. [CrossRef]
20. Ananth, S.; Vivek, P.; Saravana Kumar, G.; Murugakoothan, P. Performance of caessalpinia sappan heartwoodextract as photo sensitizer for dye sensitized solar cells. *Spectrochim. Acta Part A Mol. Bimolecular Spectrosc.* **2015**, *137*, 345–350. [CrossRef]
21. Prabu, K.M.; Anbarasan, P.M. Improved performance of natural dye sensitized solar cells (NDSSCS) using ZnO doped TiO_2 nanoparticles by sol-gel method. *Int. J. Sci. Res.* **2014**, *3*, 1740–1747.
22. Iswariya, S.; Clara Dhanemozhi, A.; Yugamica, S. Synthesis and characterization of dye sensitized solar cell using fruit extracts. *Int. Res. J. Eng. Technol. (IRJET)* **2017**, *4*, 277–285, ISSN 2395-0056.
23. Nandarapu, P.; Reshma, K.; Ganapathy, V.; Kovendhan, M.; Paul Joseph, D. Prickly pear fruit extract as photosensitizer for dye-sensitized solar cell Spectrochim. *Acta Part A Mol. Biomol. Spectrosc.* **2020**, *228*, 117686. [CrossRef]
24. Giuseppe, C.; Gaetano Di, M.; Silvia, C.; Stefano, C.; Roberto, A.; Aldo Di, C.; Carlo Alberto, B. Efficient Dye-Sensitized Solar Cells Using Red Turnip and Purple Wild Sicilian Prickly Pear Fruits. *Int. J. Mol. Sci.* **2010**, *11*, 254–267. [CrossRef]
25. Kenneth, O.; Liliya, F.; Paul, F. Preparation and performance of prickly pear (*Opuntia phaeacantha*) and mulberry (*Morus rubra*) dye-sensitized solar cells. *Sol. Energy* **2020**, *208*, 312–320. [CrossRef]
26. Prabu, K.M.; Anbarasan, P.M.; Ranjitha, S. Natural Dye-Sensitized Solar Cells (NDSSCs) from Opuntia Prickly Pear Dye Using ZnO Doped TiO_2 Nanoparticles by Sol Gel Method. *Int. J. Eng. Res. Appl.* **2014**, *4*, 2248–9622.
27. Noureddine, B.; Khalid, O.; Mohamed, A.; Mohammed, M. Dried prickly pear cactus (*Opuntia ficus indica*) cladodes as a low-cost andeco-friendly biosorbent for dyes removal from aqueous solutions. *J. Taiwan Inst. Chem. Eng.* **2013**, *44*, 52–60. [CrossRef]
28. Rauf, M.A.; Graham, J.P.; Bukallah, S.B.; Al-Saedi, M.A.S. Solvatochromic behavior on the absorption and fluorescence spectra of Rose Bengal dye in various solvents. *Spectrochim. Acta Part A* **2009**, *72*, 133–137. [CrossRef]
29. Zhang, F.; Shi, F.; Ma, W.; Gao, F.; Jiao, Y.; Li, H.; Wang, J.; Shan, X.; Lu, X.; Meng, S. Controlling Adsorption Structure of Eosin Y Dye on Nanocrystalline TiO_2 Films for Improved Photovoltaic Performances. *J. Phys. Chem. C* **2013**, *117*, 14659−14666. [CrossRef]
30. Chen, J.; Zhang, L. NH4Cl-assisted low temperature synthesis of anatase TiO_2 nanostructures from Ti powder. *Mater. Lett.* **2009**, *63*, 1797–1799. [CrossRef]
31. Laisney, J.; Rosset, A.; Bartolomei, V.; Predoi, D.; Truffier-Boutry, D.; Artous, S.; Bergé, V.; Brochard, G.; Michaud-Soret, I. TiO_2 nanoparticles coated with bio-inspired ligands for the safer-by-design development of photocatalytic paints. *Environ. Sci. Nano* **2021**, *8*, 297–310. [CrossRef]
32. Hargreaves, J.S.J. Some considerations related to the use of the Scherrer equation in powder X-ray diffraction as applied to heterogeneous catalysts. *Catal. Struct. React.* **2016**, *2*, 33–37. [CrossRef]
33. Nandhakumar, E.; Priya, P.; Selvakumar, P.; Vaishnavi, E.; Sasikumar, A.; Senthilkumar, N. One step hydrothermal green approach of CuO/Ag nanocomposites: Analysis of structural, biological activities. *Mater. Res. Express* **2019**, *6*, 95036. [CrossRef]
34. Pitchaiya, S.; Eswaramoorthy, N.; Natarajan, M.; Santhanam, A.; Asokan, V.; Ramakrishnan, V.M.; Rangasamy, B.; Sundaram, S.; Ravirajan, P.; Velauthapillai, D. Perovskite solar cells: A porous graphitic carbon-based hole transporter/counter electrode material extracted from an invasive plant species eichhornia crassipes. *Sci. Rep.* **2020**, *10*, 6835. [CrossRef] [PubMed]

35. Sundaram, M.; Kalpana, S.; Sivaganesan, V.; Nandhakumar, E. Studies on the catalytic activity of CuO/TiO_2/ZnO ternary nanocomposites prepared via one step hydrothermal green approach. *Mater. Res. Express* **2019**, *6*, 125043. [CrossRef]
36. Heiba, Z.K.; Mohamed, M.B.; Badawi, A. Structural and Optical Characteristic of Cu-Doped TiO_2 Thin Film. *J. Inorg. Organomet. Polym.* **2022**, *32*, 2853–2862. [CrossRef]
37. Kwak, C.-H.; Im, U.-S.; Seo, S.-W.; Kim, M.-I.; Huh, Y.-S.; Im, J.-S. Effects of carbon doping on TiO_2 for enhanced visible light-driven NO sensing performance. *Mater. Lett.* **2021**, *288*, 129313. [CrossRef]
38. Ramanarayanan, R.; Nijisha, P.; Niveditha, C.V.; Sindhu, S. Natural dyes from red amaranth leaves as light-harvesting pigments for dye-sensitized solar cells. *Mater. Res. Bull.* **2017**, *90*, 156–161. [CrossRef]
39. Calogero, G.; Di Marco, G.; Caramori, S.; Cazzanti, S.; Argazzi, R.; Bignozzi, C.A. Natural dye sensitizers for photoelectrochemical cells. *Energy Environ. Sci.* **2009**, *2*, 1162–1172. [CrossRef]
40. Dai, Q.; Rabani, J. Photosensitization of nanocrystalline TiO_2 films by anthocyanin dyes. *J. Photochem. Photobiol. A Chem.* **2002**, *148*, 17–24. [CrossRef]
41. Subalakshmi, K.; Senthilselvan, J.; Kumar, K.A.; Kumar, S.; Pandurangan, A. Solvothermal synthesis of hexagonal pyramidal and bifrustum shaped ZnO nanocrystals: Natural betacyanin dye and organic Eosin Y dye sensitized DSSC efficiency, electron transport, recombination dynamics and solar photodegradation investigations. *J. Mater. Sci. Mater. Electron.* **2017**, *28*, 15565–15595. [CrossRef]
42. Chien, C.Y.; Hsu, B.D. Optimization of the dye-sensitized solar cell with anthocyanin as photosensitizer. *Sol. Energy* **2013**, *98*, 203–211. [CrossRef]
43. Barichello, J.; Mariani, P.; Matteocci, F.; Vesce, L.; Reale, A.; Di Carlo, A.; Lanza, M.; Di Marco, G.; Polizzi, S.; Calogero, G. The Golden Fig: A Plasmonic Effect Study of Organic-Based Solar Cells. *Nanomaterials* **2022**, *12*, 267. [CrossRef] [PubMed]
44. Jambure, S.B.; Gund, G.S.; Dubal, D.P.; Shinde, S.S.; Lokhande, C.D. Cost effective facile synthesis of TiO_2 nanograins for flexible DSSC application using rose bengal dye. *Electron. Mater. Lett.* **2014**, *10*, 943–950. [CrossRef]
45. Jimmy, M.J.; Harun, A.M.; Rahman, M.Y.A.; Ludin, N.A. Comparative study of dye sensitized solar cell utilizing seaweed and rose Bengal sensitizer: Influence of dye concentration. *Int. J. Electrochem. Sci.* **2020**, *15*, 3219–3231. [CrossRef]
46. Manikandan, V.S.; Palai, A.K.; Mohanty, S.; Nayak, S.K. Eosin-Y sensitized core-shell TiO_2-ZnO nano-structured photoanodes for dye-sensitized solar cell applications. *J. Photochem. Photobiol. B Biol.* **2018**, *183*, 397–404. [CrossRef]
47. Yildiz, Z.K.; Atilgan, A.; Atli, A.; Özel, K.; Altinkaya, C.; Yildiz, A. Enhancement of efficiency of natural and organic dye sensitized solar cells using thin film TiO_2 photoanodes fabricated by spin-coating. *J. Photochem. Photobiol. A Chem.* **2019**, *368*, 23–29. [CrossRef]
48. Richhariya, G.; Kumar, A. Performance evaluation of mixed synthetic organic dye as sensitizer based dye sensitized solar cell. *Opt. Mater.* **2021**, *111*, 110658. [CrossRef]

Disclaimer/Publisher's Note: The statements, opinions and data contained in all publications are solely those of the individual author(s) and contributor(s) and not of MDPI and/or the editor(s). MDPI and/or the editor(s) disclaim responsibility for any injury to people or property resulting from any ideas, methods, instructions or products referred to in the content.